Aerosol and Air Quality Research, 17: 2780–2790, 2017

ISSN: 1680-8584 print / 2071-1409 online
doi: 10.4209/aaqr.2017.05.0190

Surface Indices of Wind, Stability, and Turbulence at a Highly Polluted Urban Site in Santiago, Chile, and their Relationship with Nocturnal Particulate Matter Concentrations

Ricardo C. Muñoz[1*], Marcelo J. Corral[2]

[1] *Department of Geophysics, University of Chile, Santiago, Chile*
[2] *Ministerio del Medio Ambiente, Santiago, Chile*

ABSTRACT

The local meteorological factors of the cold season nocturnal particulate matter (PM) air quality problem in the western urban area of Santiago City are documented and analyzed by means of three years of multi-level temperature and turbulence measurements performed in-situ on a 30 m meteorological tower. For the 20–23 LT period in which the highest PM concentrations commonly occur, high prevalence of low wind and low vertical turbulence conditions are found. With wind speeds less than 1 m s^{-1}, the frequency of calms and the intensity of meandering increase, although the highest PM concentrations are associated more to meandering than to purely calm conditions. In terms of the stability of the near surface layer, while there is a general association between high PM concentrations and high stability, the most extreme PM event in the period occurred with an intermediate value of stability probably affected by the presence of mid-tropospheric clouds. Using a nocturnal vertical height scale based on the stability and the surface turbulent heat flux to compute a nocturnal ventilation factor (VF), a marked inverse relationship between VF and PM concentrations is documented. The prevalence of low winds and high meandering in this sector of Santiago is hypothesized to be related to the local topography that precludes the development of the weak but persistent drainage surface winds observed at other sites of the city. Further investigation of this very stable atmospheric boundary layer is deemed necessary for improving the numerical models used in forecasting and managing the air pollution problem of Santiago.

Keywords: Urban air pollution; Meteorological factors; Meteorological tower; Santiago; Chile.

INTRODUCTION

Urban air quality problems arise commonly from a combination of large emission rates of air pollutants related to urban activity and meteorological factors affecting their transport and dispersion. Discerning the meteorological ingredients of a given urban air pollution problem is important because: 1) it may shed light on the nature of the problem, for example, by elucidating whether it is caused by local sources or it is due to transport from elsewhere (e.g., Yu *et al.*, 2004; Rasheed *et al.*, 2015); 2) it helps in forecasting the possible occurrence of high-concentration episodes, by providing the key meteorological variables to look after in the forecasts (e.g., Ryan *et al.*, 2000; Pérez and Gramsch, 2016); 3) it is crucial in the validation of numerical meteorological- dispersion-chemistry models, in which errors in emissions, meteorology, and chemistry must be properly disentangled, if they are to be useful in forecast or impact assessment studies (e.g., Hogrefe *et al.*, 2007; Yegorova *et al.*, 2011); 4) it aids the design and evaluation of strategies for the short-term management of air pollution problems (e.g., Jorquera and Castro, 2010; Mullins and Bharadwaj, 2015); and 5) it helps in the assessment whether concentration trends respond to improvements in emission controls or are the result of meteorological variability (e.g., Wise and Comrie, 2005; Sax *et al.*, 2007; Reddy and Pfister, 2016). For these reasons, most urban air pollution networks include some meteorological measurements, although few go beyond standard meteorological sensors measuring wind speed and direction near the surface, and perhaps other variables like temperature and relative humidity. The present contribution describes and discusses more advanced measurements specifically designed to provide a better understanding of the local meteorological factors relevant to the particulate matter (PM) problem in the western urban sector of Santiago City in Chile, South America.

The city of Santiago (33.5°S, 70.6°W, 550 m above sea level [ASL], ~7 Million inhabs.) is located at the floor of a 30 × 90 km valley confined by the Andes Cordillera to the east (altitudes above 4,000 m ASL), the Coastal Range to

[*]Corresponding author.
Tel.: 56-2-29784305; Fax: 56-2-26968686
E-mail address: rmunoz@dgf.uchile.cl

the west (altitudes above 1,000 m ASL), and zonal hill chains to the north and south that limit ventilation of the air mass in the valley (Fig. 1(a)). Furthermore, its subtropical location makes the regional climate to be dominated by the semi-permanent South-East Pacific Anticyclone (inset in Fig. 1(a)), providing for a high prevalence of very stable conditions in the lower troposphere (Rutllant and Garreaud, 1995). The large emissions of the big city, together with the topographic constraints and the climatological setting, combine to produce a well known severe air pollution problem, which in winter takes the form of frequent exceedances of aerosol standards, both in terms of particulate matter with aerodynamic size less than 10 μm (PM_{10}), and less than 2.5 μm ($PM_{2.5}$) (Koutrakis *et al.*, 2005; Jhun *et al.*, 2013). Emission inventories and source apportionment studies point to transport emissions and residential sources as very significant sources of PM in Santiago (U. of Santiago, 2014; Barraza *et al.*, 2017). In particular, residential wood-burning for heating may be an important local source of PM in the study area during winter nights.

Under the climatological and topographic setting described above, the mean surface circulation regime in Santiago corresponds to a valley-mountain breeze system that produces south-westerly winds in the afternoon and weak easterly winds in the night (Garreaud and Rutllant, 2006). The meteorological factors of the air pollution problem in Santiago have been studied since the 1960's (Rutllant and Garreaud, 1995; and references therein). In particular, Rutllant and Garreaud (1995) categorized the synoptic and sub-synoptic conditions favoring the occurrence of episodes of high air pollutant concentrations in Santiago. The most frequent condition associated to air pollution episodes in Santiago is characterized by a mid-tropospheric ridge approaching Chile from the west, a migratory surface high pressure system crossing towards Argentina to the south of Santiago and the subsequent development of a coastal low in central Chile, all of which strengthens the subsidence in the western flank of the Andes Cordillera and enhances the lower tropospheric stability over Santiago valley (Garreaud and Rutllant, 2006). More recently, Ragsdale *et al.* (2013) and Barrett *et al.* (2012) documented the influence of the Madden-Julian oscillation on the air quality of Santiago. At a more local scale and closer to the scale addressed in the present work, Gramsch *et al.* (2014) studied the influence of the thermal stability and other local meteorological factors on black carbon concentrations in Santiago. Due to the lack of continuous observations of vertical profiles of meteorological variables in Santiago, however, the stability characterization had to be performed with limited datasets: 3 months of temperature profiles measured by commercial aircraft operating at Santiago's airport, which provided only two morning soundings every day during the period, and 45-days of temperature measurements at the top and base of a 300-m hill in the valley. Finally, Corral (2014) documented the relationship between lower-tropospheric stability and particulate matter concentrations in Santiago using data gathered in year 1999 by a LAP-RASS system and a micrometeorological tower, both located in the south-eastern sector of Santiago. The former equipment provided hourly measurements of temperature from 110 m up to about 1,000 m above ground level (AGL) with 60 m vertical resolution. The tower, on the other hand, had temperature sensors located at 2, 8 and 22 m AGL. The present work can be considered an extension of Corral (2014) taking advantage of newly available and more extended observations of near-surface stability and turbulence at a point closer to where the highest particulate matter concentrations occur.

The objectives of the paper are thus 1) to describe the variability of near-surface meteorological indices at a polluted urban site based upon observations on a 30 m tower with temperature measurements at 2, 10, and 30 m, and turbulence measurements with an ultrasonic anemometer at 10 m AGL, and 2) to quantify the relationship between particulate matter concentrations at the site and meteorological indices describing surface wind, stability and turbulence. The next section describes the measuring sites and available data. Then, the results are presented, both in terms of a description of the variability of the relevant meteorological indices and their relationship with particulate matter concentrations. The last sections discuss the results, put them in the context of previous studies and assess their significance.

SITE AND DATA

Fig. 1 shows a close-up of the topographic relief around the urban area of Santiago and the location of the current official air pollution monitoring stations in the area. The stations provide hourly measurements of criteria air pollutants like PM_{10} and $PM_{2.5}$ particulate matter, sulphur dioxide, carbon monoxide, and ozone, as well as meteorological parameters (wind speed and direction, temperature and relative humidity) measured at 10 m AGL (Gramsch *et al.*, 2006). As mentioned before, the main air pollution problem of Santiago during the cold season is related to high particulate matter concentrations, a problem that is commonly more acute in the western sector of the city, namely the area represented by monitoring stations O and R (Gramsch *et al.*, 2006; Pérez and Gramsch, 2016). Fig. 2(a) shows the diurnal distribution of PM_{10} concentrations averaged at stations O and R for the months of May to August. We restrict our analyses to this cold season period to avoid introducing in our correlations the effect of the strong annual cycles present in both the meteorological and the concentration variables. The diurnal cycle of PM_{10} shows conspicuous peaks in the morning and in the first hours of the night, a pattern that has been discussed by Muñoz (2012). Of more interest for the present study is the observation that the highest values of PM_{10} (as represented by the 95% percentile) show a more significant increase with respect to the average values during the evening and early night hours as compared to the rest of the day, suggesting that these hours are important in determining the occurrence of high- PM_{10} episodes in this area.

In order to better characterize the local meteorological factors that may influence the occurrence of high PM concentrations in this area, in year 2013 the Ministry of the Environment procured the installation of a 30 m tower at a site located about 0.7 km south of station O and 1.7 km

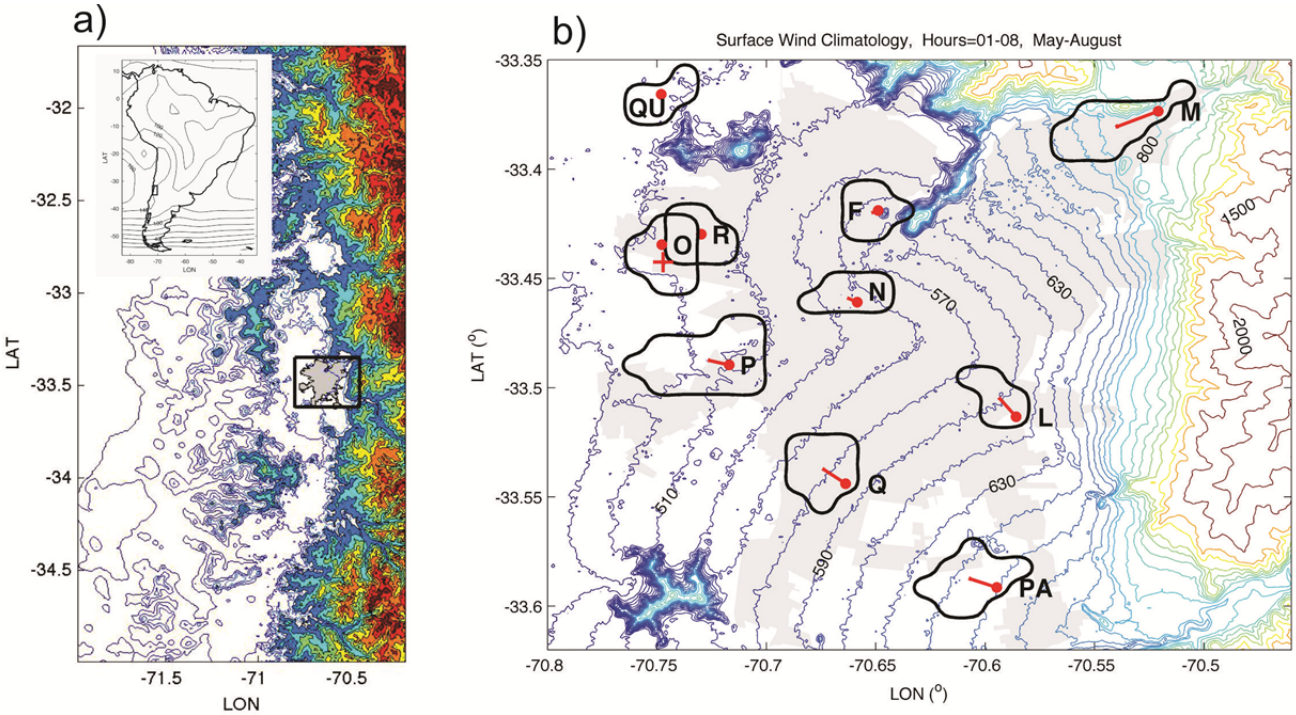

Fig. 1. a) Regional topography around Santiago city (shaded region). Line contours from 0 to 800 m ASL every 200 m, colored contours from 1,000 m ASL upwards every 500 m. Inset shows location of the region in South America, together with the 1985–2014 averaged 1000-hPa geopotential height field obtained from NCEP/NCAR Reanalysis (Kalnay *et al.*, 1996). Black rectangle shows location of region of panel b). b) Topographic map around Santiago city urban area (shaded region). Contour lines every 20 m from 450 to 750 m ASL, every 50 m from 800 to 950 m ASL, every 100 m from 1,000 to 1,200 m ASL, and every 500 m above 1,500 m ASL. Red circles show locations of the air quality monitoring stations of Santiago. Red cross close to station O shows the location of the 30-m meteorological tower. Red lines emerging from each circle describe the direction and magnitude of the vector-averaged 10 m wind. Scaling of the red lines corresponds to the 30-minute displacement associated to the wind speed. Black lines surrounding each station demarcate the region where 80% of all the 30-minute displacements fall. Only hours between 01 and 08 LT and for the months from May to August are considered in this climatology. Database used to construct the wind climatology covers different multi-year periods in the range from 2004 to 2016, depending on the station.

southwest of station R (point marked with a red cross in Fig. 1). The full suite of instruments installed in the tower and their averaging times is presented in Table 1. Of particular interest for this study is the availability in the tower of 3-D ultrasonic anemometers providing for the first time direct measurements of turbulence levels in the area. Additionally, the three temperature sensors installed at 2 m, 10 m, and 30 m AGL, provide a measure of the stability near the surface.

In Fig. 2, panels b), c), and d) show the diurnal distributions of 10 m wind speed, standard deviation of the vertical velocity (SW) at 10 m, and stability in the 2–10 m layer, respectively. Marked diurnal cycles are evident for all these variables. Mean wind speeds maximize around hours 15–16 LT, decreasing rapidly afterwards. It is noteworthy that after 19 LT the median wind speed is lower than 1 m s^{-1} and after 23 LT even the upper quartile remains below 1 m s^{-1} for the rest of the night until 9 LT in the morning. This confirms the high prevalence of near calm conditions in this area of the city during the cold season. The intensity of vertical turbulence (Fig. 2(c)) increases rapidly in the morning hours presumably in connection to the heating of the surface by solar radiation. Maximum values of SW in the typical range of 0.3–0.5 m s^{-1} are attained also around 15 LT, declining until 22 LT and remaining generally smaller than 0.1 m s^{-1} for the rest of the night. The lowest 5-percentile of SW drops to values less than 0.1 m s^{-1} around 17 LT, showing that on some occasions vertical dispersion of pollutants can be reduced quite early in the evening. Finally, the diurnal pattern of surface stability (Fig. 2(d)) shows unstable conditions between 8 and 17 LT, a transition period between 17 and 21 LT, and generally stable conditions thereafter. The upper 5-percentile in stability shows that occasionally the largest stabilities are found in the transition hours between 18 and 21 LT.

In order to explore the local meteorological factors affecting PM concentrations in the area, we have defined several indices pertaining to the local conditions of winds, turbulence and stability, as well as to PM_{10} concentrations. Three time periods have been defined, marked as P0, P1 and P2 in Fig. 2(a). Period P0, denoting averages for hours 12–15 LT, represents low-concentration cases associated with the phase of the diurnal cycle with high winds and enhanced vertical turbulence. Period P1 averages over

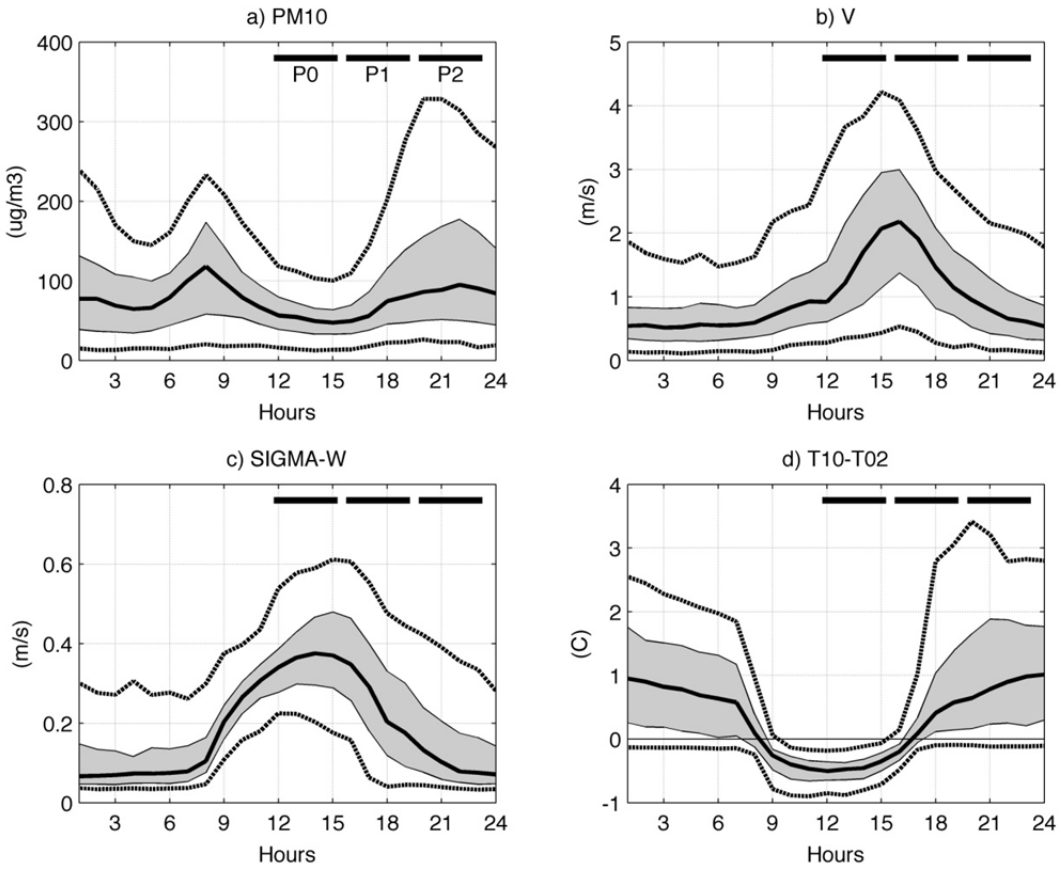

Fig. 2. Diurnal variability of PM_{10} and local meteorological variables in the west area of Santiago city for the months of May-August of years 2014–2016. a) Diurnal variability of hourly PM_{10} concentrations averaged for stations O and R showing the median (bold line), inter-quartile range (gray area) and 5% and 95% percentiles (dotted lines). b) As a) but for wind speed at 10 m AGL. c) As a) but for the standard deviation of vertical velocity at 10 m AGL for years 2014–2015. d) As a) but for the temperature difference between 10 m and 2 m AGL. Bold lines marked as P0, P1 and P2 in panel a) show the time averaging periods chosen to compute meteorological and concentration indices.

Table 1. Meteorological sensors on the 30-m tower.

Variable	Make/Model	Heights (m AGL)	T1/T2/T3[(1)] (s)
Turbulence[(3)]	RM Young/81000	10, 30	300/1/0.25[(2)]
Temperature	RM Young/Platinum	2, 10, 30	300/1/-
Wind	RM Young/05103	10	60/1/-
Temp./Rel.Hum.	Vaisala/HMP155A	2	60/1/-
Precipitation	Texas Electronics/TE525mm	2	60/1/-
Atm. Pressure	Vaisala/PTB110	2	60/1/-
Net radiation	Kipp&Zonen/NR-LITE 2	2	60/1/-

[(1)] T1: datalogger averaging time; T2: datalogger scanning time; T3: sensor measuring time.
[(2)] The ultrasonic anemometers measure data every 0.25 s but they average 4 values to provide 1 s averages to the datalogger.
[(3)] Both ultrasonic anemometers (UA) failed in year 2016. The UA at 30 m had intermittent problems in years 2014–2015, therefore the paper uses only turbulence data of the UA at 10 m for years 2014–2015.

hours 15–19 LT and corresponds to the transition conditions of decreasing winds and turbulence and increasing stability. Finally, period P2, corresponding to averages of hours 20–23 LT, encompasses the time period in which the highest PM concentrations typically occur at these two sites. While most of our analysis focuses on period P2, some discussion of conditions in the previous periods will be made.

For each of the above defined time periods, particulate matter concentrations are characterized by the IPM10 index, defined by the simple 4-hour average of PM_{10} concentrations at stations O and R. An analogous index based on $PM_{2.5}$ concentrations is highly correlated with IPM10 ($r \sim 0.91$ for period P2), so that local meteorological controls on both aerosol types are not easily distinguishable. Three indices

describing local winds were defined. The first index, V, is simply the magnitude of the 10 m vector-averaged wind in the period. It represents the net movement of the local air mass in the 4-hour period. The second index, ICF, characterizes the fraction of time in which near-calm conditions prevail. It is defined as the time fraction of the 4-hour period in which the 1-minute wind speed data is less or equal than 0.1 m s^{-1}, the latter corresponding to the threshold wind speed measured by the R.M. Young 05103 anemometer. Finally, the third wind index, IM, attempts to describe the meandering character of the wind field. It is defined as the ratio between the magnitude of the vector averaged wind and the average of the wind speed magnitude (also called a constancy index by Mahrt, 2007). It is a non-dimensional quantity always less or equal than 1, with smaller values for meandering cases. Two versions of this index are used: IM computed over 1-hour periods and then averaged over the 4-hour period of the analysis, and IM4h, computed once over the full 4-hour period of interest.

Turbulence and stability where characterized by the ISW and ISTAB indices, defined simply as the averaged standard deviation of vertical velocity at 10 m AGL, and the averaged vertical temperature gradient in the 2–10 m layer, respectively. A bulk Richardson number, Rb, was computed following Mahrt *et al*. (2012). Another meteorological index useful in the assessment of cloudiness conditions during the night, the IRNET index, was computed as the average of the radiative flux measured by the net radiometer in each period. Finally, we use the current dataset to explore also the relationship between PM_{10} concentrations and a ventilation factor index (VF), computed as the product of V and a mixed layer height estimate, H. In a simple box-model approach to air pollution problems, concentrations are inversely related to the ventilation factor, a concept that has been applied to the Santiago case in various forms (Rutllant and Garreaud, 1995; Jorquera, 2002; Pérez and Gramsch, 2016). Due to the lack of routine observations in the vertical in Santiago, however, the values of H in the ventilation factor have been only estimates based on limited data or in numerical model results. In the present case, we compute VF for period P0 estimating H with the daytime mixed layer height derived from observations in Santiago with a lidar ceilometer (located very close to station N in Fig. 1) as described by Muñoz and Undurraga (2010). For the nocturnal period P2, we estimate H using turbulent and stability data of the 30-m tower by

$$H = \left(\frac{-2 \int \overline{w'T'} dt}{\Gamma} \right)^{1/2} \quad (1)$$

where $\overline{w'T'}$ is the kinematic turbulent surface heat flux computed as the covariance between turbulent fluctuations of vertical velocity, w', and sonic temperature, T', measured by the ultrasonic anemometer at 10 m AGL, the integral covers the period from 17 to 23 LT, and Γ corresponds to ISTAB. The rationale behind Eq. (1) is the assumption that the cooling due to the turbulent heat flux at the surface cools an inversion layer of height H with temperature gradient, Γ, starting from a near isothermal temperature profile at the beginning of the night (Stull, 1988; p. 504). Radiative and advective influences in the development of the nocturnal inversion are not considered in Eq. (1), which is discussed later when nocturnal H values are used to assess the relationship between PM_{10} and ventilation factors.

RESULTS

The three upper panels in Fig. 3 describe the wind-related indices for period P2. Fig. 3(a) presents the scatter diagrams of ICF and IM with respect to V. At this time of the day (20–23 LT), about 67% of V values are less than 1 m s^{-1}. The latter value appears to be a threshold above which meandering and calms are infrequent (IM ~1 and ICF ~0). In contrast, with V < 1 m s^{-1} the index ICF can be as high as 0.7, indicating that in extreme cases 70% of the 4-hour period has 1-minute winds below the anemometer threshold of 0.1 m s^{-1}. At the same time, with V < 1 m s^{-1}, the meandering index IM can be as low as 0.3, indicating that the net hourly transport can be 30% of the actual movement of the air mass around the measuring point. While both calms and meandering appear to increase with V < 1 m s^{-1}, ICF and IM are not much correlated as shown by Fig. 3(b), suggesting that these two traits of low-wind conditions are more or less independent of each other at this site. Finally, Fig. 3(c) explores the sensitivity of the meandering index upon the time period over which it is computed. At an hourly timescale, IM is rarely below 0.5, but when computed over the full 4-hourly period, IM4h can reach values as low as 0.1. This suggests the presence of very low-frequency meandering, which could be a factor in the high concentrations of air pollutants at this site.

Considering that vertical turbulence is controlled by a mechanical factor related to wind speed and by a buoyant factor associated to the stability of the temperature profile, the lower panels in Fig. 3 explore the observed relationships between ISW and V (Fig. 3(d)), and between ISW and ISTAB (Fig. 3(e)), for the three time periods under consideration: P0 (blue dots), P1 (red dots), and P2 (green dots). As expected, ISW and V are positively correlated, with stability playing a modulating role in this relationship. This latter effect is evident when comparing the ISW-V relationship in period P0 (mostly under unstable conditions, according to Fig. 3(e)) with that in periods P1 and P2 (mostly under stable conditions). For the same V values, the stable periods have lower ISW values as compared to those in the unstable period P0, a difference that is more pronounced in the lowest wind cases, in which under stable conditions vertical turbulence tends to zero while under unstable conditions a significant variability of the vertical wind speed persists even with V ~0, presumably due to convective production of turbulence. Indeed, it is noteworthy that in the stable period P2, 47% of cases have ISW less than 0.1 m s^{-1}, showing the prevalence of very weak turbulence at the site. Fig. 3(e), on the other hand, shows the relationship between vertical turbulence and stability. Although a general association between high stability and low vertical turbulence is observed, it will be of

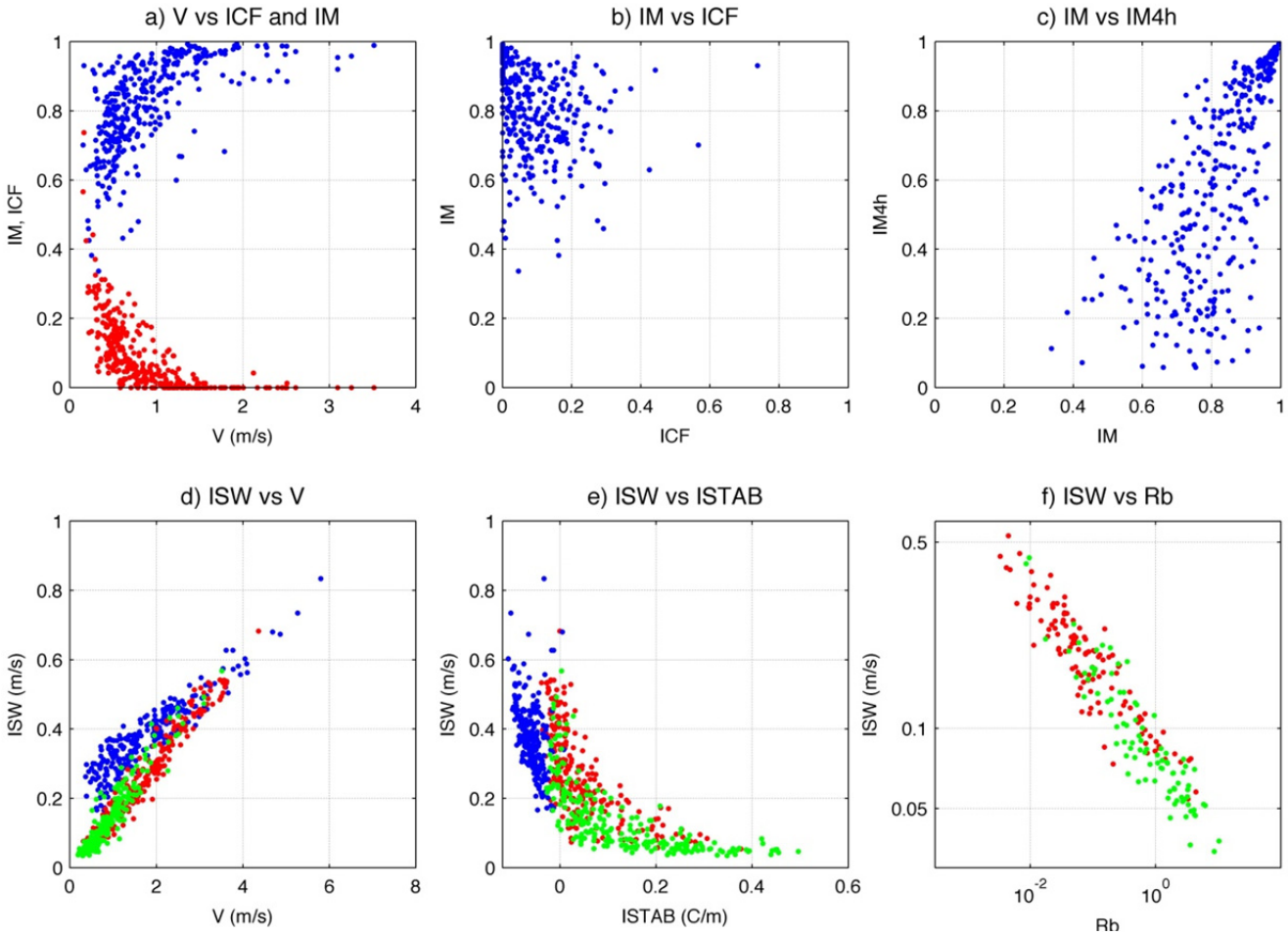

Fig. 3. Wind speed and vertical turbulence indices measured at meteorological tower. a) Scatter diagram between meandering index (IM, blue points), calm fraction index (ICF, red points) and wind speed (V) for period P2 (20–23 LT). b) Scatter diagram between IM and ICF for period P2. c) Scatter diagram between 1-hour meandering index (IM) and 4-hour meandering index (IM4h) for period P2. d) Scatter diagram between vertical turbulence index (ISW) and wind speed V for periods P0 (blue), P1 (red) and P2 (green). e) As d) but for the scatter diagram between ISW and the stability index ISTAB. f) As d), but for the log-log scatter diagram between ISW and bulk Richardson number Rb for stable conditions.

interest for a subsequent discussion to notice that low ISW values can exist under a wide range of stability in the temperature profile. For example, ISW ~0.1 m s^{-1} coexists with ISTAB ranging from 0 to 0.4 C m^{-1} in period P2. Finally, the influence of mechanical and stability factors in turbulence is commonly described by the computation of non-dimensional parameters like the Richardson number, which is explored in Fig. 3(f). There, the log-log scatter diagram between ISW and a bulk Richardson number, Rb, for stable conditions is presented, confirming indeed an inverse relationship between vertical turbulence and the Richardson number.

The upper panels in Fig. 4 show the relationship between IPM10 and the three wind indices for period P2 in which the largest particulate matter concentrations commonly occur. The scatter diagram of IPM10 and V shown in Fig. 4(a) clearly demonstrates that the highest PM concentrations (IPM10 > 300 μg m^{-3}) in the evening at these sites can occur only with low mean wind speed values (V < ~1 m s^{-1}), while mean wind speeds larger than 1.5 m s^{-1} appears to be sufficient to have IPM10 < 100 μg m^{-3}. With low wind speeds being a factor for high PM concentrations, Figs. 4(b) and 4(c) explore the roles of calms frequency and meandering, respectively, because low V values can be associated to both traits of low wind conditions (see Figs. 3(a) and 3(b)). Interestingly, the scatter diagram between IPM10 and ICF in Fig. 4(b) shows that the highest PM concentrations (IPM10 > 350 μg m^{-3}) are observed with rather modest values of ICF (ICF < 0.2). At the same time, large ICF values (ICF > 0.4) are associated with only medium or low IPM10 values (< ~300 μg m^{-3}). This suggests that purely calm conditions are not conducive of high PM_{10} values at these sites. On the other hand, Fig. 4(c) shows that the highest IPM10 values occur with medium or low values of IM4h, suggesting that meandering is a factor needed for the occurrence of high PM concentrations. A plausible explanation for these observations is that indeed purely calm conditions would only produce high concentrations if a significant pollutant source exists very close to the monitoring station (which location protocols for these monitoring

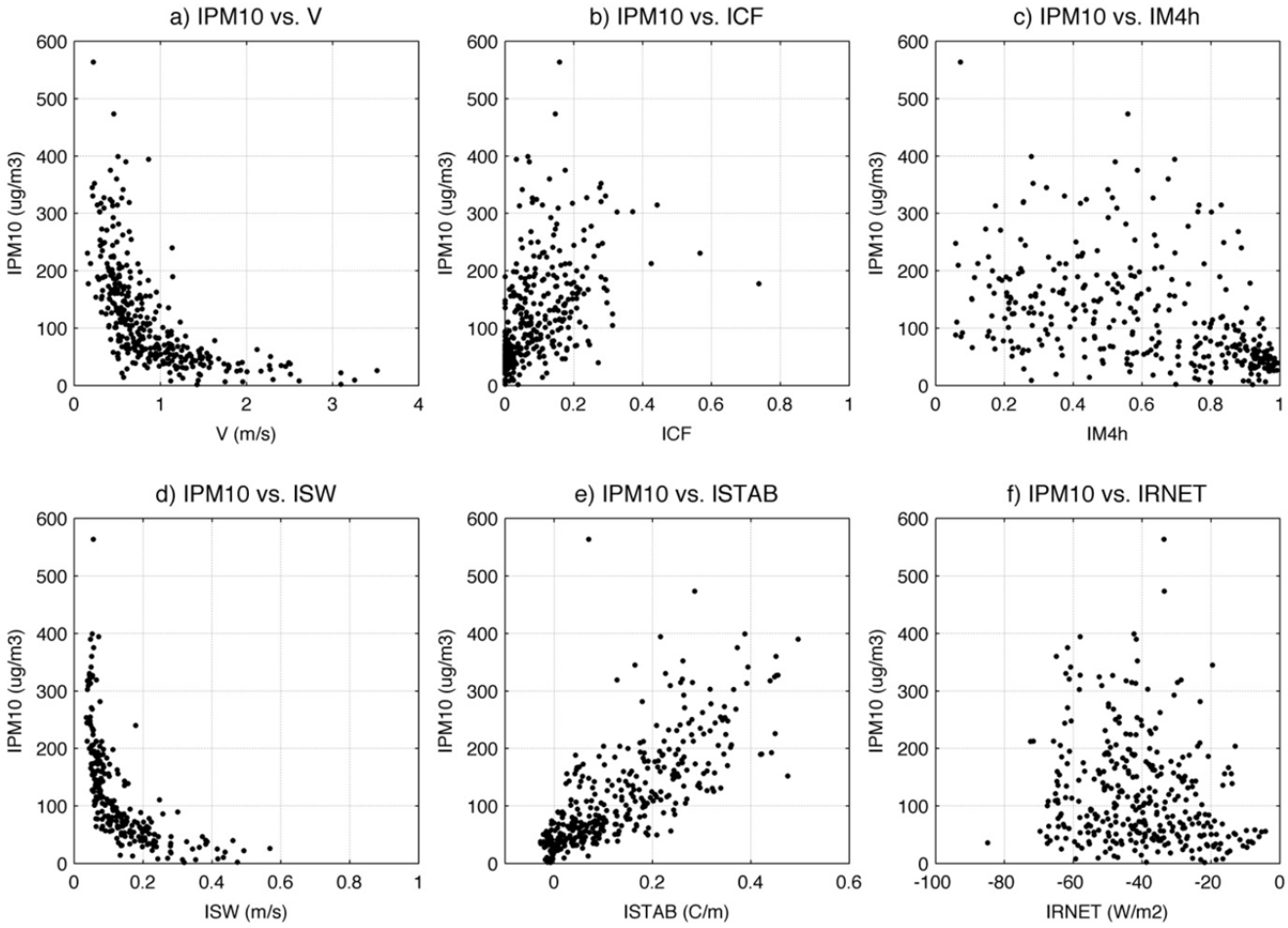

Fig. 4. PM_{10} index (IPM10) versus local meteorological indices for period P2 (20–23 LT). a) Scatter diagram between IPM10 and wind speed index V. b) Scatter diagram between IPM10 and calm fraction index ICF. c) Scatter diagram between IPM10 and 4-hour meandering index IM4h. d) Scatter diagram between IPM10 and vertical turbulence index ISW only for years 2014–2015. e) Scatter diagram between IPM10 and stability index ISTAB. f) Scatter diagram between IPM10 and net radiation index IRNET.

stations try to avoid), so that some meandering is required in order to transport PM from nearby sources, like residential wood-burning and local traffic, to the stations.

The association between IPM10 and the intensity of the vertical turbulence is explored in Fig. 4(d). As expected, a necessary condition for high PM concentrations appears to be a reduced turbulence level, with ISW< 0.1 m s^{-1}, while ISW > 0.2 m s^{-1} is sufficient to have concentrations less or equal than 100 μg m^{-3} in period P2. A more surprising result is the association between PM concentrations and near surface stability as presented in Fig. 4(e). While there is a general positive relationship between IPM10 and ISTAB, the most extreme value of IPM10 in the period occurred not with very high stability but with the ISTAB index in its middle range of variation. Thus, although this extreme IPM10 case had very low wind speeds (Fig. 4(a)) and vertical turbulence intensity (Fig. 4(d)), its surface stability was not particularly high. A possible explanation for this observation is aided by Fig. 4(f), in which the association between IPM10 and the net radiative index IRNET is shown. Net radiation during the night is typically negative, with large magnitudes when clear skies prevail and values closer to zero in cloudy conditions. Fig. 4(f) shows that although in general clear nights (large negative IRNET values) allow for larger PM_{10} concentrations, the most extreme IPM10 case occurred with a medium value of IRNET, suggesting that this night had a partial cloud cover at some altitude, a condition confirmed by the inspection of infrared GOES satellite imagery (not shown). Thus, the highest PM_{10} concentration at these sites during the early night appear related to low winds, meandering, very low vertical turbulence and partial cloudiness.

Finally, we test in Fig. 5 the relationship between PM_{10} concentrations and the ventilation factor index (VF) combining wind speed and estimates of the mixed layer height. The statistical distributions of the latter during the night and the day are shown in panels a) and b) of Fig. 5, respectively. During the night, the estimate of H based on the stability of the surface inversion and the surface turbulent heat flux measured by the ultrasonic anemometer (Eq. (1)), ranges typically between 10 and 100 m AGL, while during the afternoon the ceilometer-derived mixed

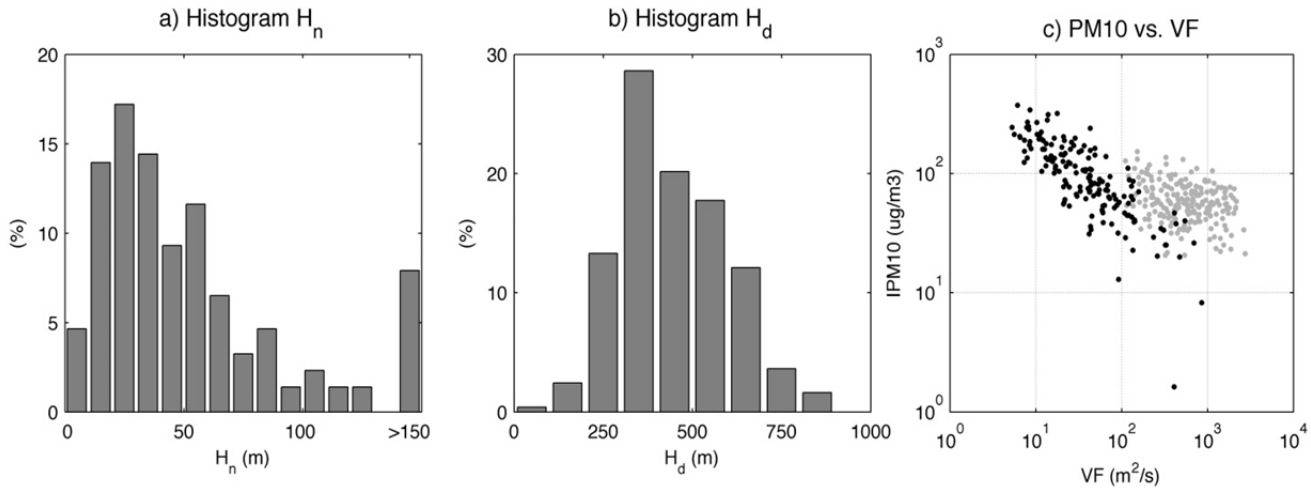

Fig. 5. Frequency histograms of a) nocturnal height scale Hn, and b) diurnal height scale Hd. c) Log-log scatter plot between diurnal (gray circles) and nocturnal (black circles) ventilation factor (VF) and PM_{10} indices. In the nocturnal cases of c), only cases in which the average $\overline{w'T'}$ was less than –0.002 K m s^{-1} were considered, so that turbulent cooling of the inversion layer was significant and Hn was a relevant height scale.

layer height varies typically between 100 and 700 m AGL. Fig. 5(c) shows that an inverse relationship between IPM10 and VF is more evident for the nocturnal condition, in which a correlation coefficient of –0.8 is attained between the two variables. We have left out of consideration cases in which the turbulent surface heat flux was extremely low and the H scale of Eq. (1) was not a relevant scale for the mixing, as attested by the wild variability these cases introduced in the scatter diagram of Fig. 5(c) (not shown). Presumably, in these cases the development of the stability profile and the nocturnal cooling may be controlled by factors other than turbulence, such as, for example, radiative processes. In contrast to the nocturnal points in Fig. 5(c), the afternoon correlation between IPM10 and VF is much weaker (r ~–0.3), suggesting that at this time advection or secondary aerosol formation may be more important in controlling concentrations as compared with local surface emissions.

DISCUSSION

The high frequency of low and near-calm winds in this sector of Santiago described above is hypothesized to be conditioned by the topography. This is sustained by an exploratory climatological analysis of the nocturnal cold-season hourly winds measured at all stations of Santiago's air pollution monitoring network shown in Fig. 1(b). Using these hourly winds we computed 30-minute displacement vectors. Their vector average is shown in Fig. 1(b) as red lines emerging from each station. It is remarkable how these mean winds show a clear association to the topography represented by the high resolution altitude contour lines. Indeed, southern and eastern stations located in an area where the topography has a slope of about 1% have mean winds with small but non-zero magnitudes and directions closely oriented along the topographical gradient. Of some interest is station M, located at a point where the Mapocho river canyon exits towards the Santiago valley. Gramsch *et al.* (2006) showed that nocturnal PM concentrations at this site are significantly smaller as compared to the rest of the monitoring stations, a fact they hypothesized to be related to a reduced stability in this higher-altitude station. The wind climatology in Fig. 1 suggests that the location of station M favours stronger nocturnal drainage winds that may preclude the rising of nocturnal PM concentrations in this area. In contrast, stations O and R located where the topographic slope is significantly smaller, have mean winds close to zero. The variability of the winds is illustrated by the black bold contours surrounding each station, which demarcate the area where 80% of the 30-minute displacements fall. Again, the variability is closely related to the topography: while in the southern and eastern stations the variability area is clearly shifted towards the down-slope direction, in stations O and R the variability is quite symmetrical around the station, confirming that in this sector the topographic slope is not large enough to induce a significant and persistent transport during night hours in the cold season. This influence of the topography in the climatology of the surface nocturnal winds suggests that the mechanism of drainage or katabatic winds (Whiteman, 1990) is of importance in the Santiago valley.

The observational database presented in this work has also made possible for the first time to perform an empirical evaluation of the degree in which a ventilation factor index explains the variability of surface PM concentrations in Santiago. The best results are found for the nocturnal concentrations, whose inter-daily variability has a correlation coefficient of –0.8 with the ventilation factor, the latter using a vertical height scale derived from the stability and the surface turbulent heat flux. Furthermore, the nocturnal relationship between IPM10 and VF in Fig. 5(c) can be used to compute an estimate for the surface emission rate of PM_{10}. The equilibrium concentration, C_*, of a non reactive pollutant computed with a well mixed box model with incoming clean air is simply (Arya, 1999; p. 278):

$$C_* = \frac{QL}{HV} \quad (2)$$

where Q is the surface emission rate, L is a size scale of the emission area, H is the mixed layer height and V is the wind speed (HV being the ventilation factor). The non-reactive assumption in underlying Eq. (2) can be justified in the case of PM during night in Santiago by the measurements of Gramsch *et al.* (2016), who found that during nocturnal air pollution episodes in Santiago, the contribution of secondary aerosol to PM concentration was minor. The nocturnal points in Fig. 5(c) suggest that a representative value of ventilation factor HV ~50 m^2 s^{-1} is associated with a typical concentration C_* ~100 μg m^{-3}. Assuming L ~10,000 m for the size of the local emission area, Eq. (2) allows for an estimate of the surface PM_{10} emission rate Q ~0.5 μg m^{-2} s^{-1}. Current emission inventories of PM_{10} for Santiago estimate an emission of about 6,600 Ton yr^{-1} (U. of Santiago, 2014), which distributed uniformly and constantly over a 30 × 30 km urban area produces a 0.2 μg m^{-2} s^{-1} surface emission rate. While this latter value and our own estimate may well have an order of magnitude of uncertainty, the fact that the two figures are of the same order is reassuring.

CONCLUSIONS

In this work we have assessed the relationship between particulate matter (PM) concentrations in the western urban area of Santiago city and newly available local measurements of winds, turbulence and stability, with emphasis in the early-night cold-season conditions in which this sector of the city is commonly affected by very high PM levels. The occurrence of very low winds (67% of cases have V < ~1 m s^{-1} averaged over hours 20–23 LT in the months from May to August) in the area appears to be a necessary factor for high PM concentrations, confirming the findings by Gramsch *et al.* (2006) and Gramsch *et al.* (2014). Beyond the influence of the mean wind speeds on PM concentrations, the newly available data has allowed us to explore the impact of meandering and the occurrence of calm conditions. While both conditions increase their frequency with wind speeds less than 1 m s^{-1}, they are rather independent between them. Our analysis shows that high PM_{10} concentrations require some meandering at multi-hour time scales, while purely calm conditions are not associated to the highest PM concentrations.

In terms of turbulence intensity, measurements with the ultrasonic anemometer at 10 m show that between 20 and 23 LT the standard deviation of vertical velocity (SW) is highly correlated with wind speed so that the high prevalence of low wind speeds is paralleled by high frequency of very weak vertical turbulence (47% of cases have averaged SW < 0.1 m s^{-1}). The relationship of SW with surface stability, on the other hand, is not as direct. While the stability in the 2–10 m layer can become larger with smaller SW, there are many cases in which both SW and the stability are small. Using the classification scheme of nocturnal conditions defined by Mahrt *et al.* (2012), 26% of the 20–23 LT averages can be categorized as "stronger winds" cases, and 22% of cases fall in the category of "near calm winds with strong stratification". In the near-calm regime, these authors point to the importance of submesoscale motions with length scales less than 2 km (Mahrt, 2014) which in the current site may be associated to the meandering described above. These submesoscale motions may also be related to complex aerosol layers that have been documented to appear in the Santiago boundary layer during the evening transition in the cold season (Muñoz and Alcafuz, 2012; Escribano *et al.*, 2014). The exact nature of this phenomenon, however, has not been fully elucidated yet.

The fact that under weak turbulence conditions the near-surface stability can vary over a wide range, suggests that stability is affected by factors other than the turbulence, for example, by the humidity profiles or cloudiness conditions that modify the radiative cooling profile. In fact, for the 3-year database analyzed here, the case with highest PM_{10} concentrations in hours 20–23 LT occurred with a medium value of surface stability presumably associated to the presence of a mid-tropospheric cloud layer.

The results presented in this contribution show that local meteorological conditions play a significant role in the occurrence of high PM concentrations in the western section of Santiago city during cold season nights. This role is not a full determination of the concentration levels, however, as variability in emission rates is certain to play an important role as well. Main meteorological factors allowing for high PM concentrations are weak vertical turbulence and low winds, the latter also characterized by high meandering at 4-hourly time scales. These traits of the local wind field are presumably related to the small topographic slope of the surrounding terrain and the weak synoptic pressure gradients prevailing during pollution episodes. From a theoretical point of view, Mahrt (2014) showed that the understanding of the stable atmospheric boundary layer under such conditions is far from complete, posing basic questions like the relationship of submesoscale motions to surface conditions, topography and larger scale forcing, the role of waves, submesoscale motions and drainage flows in affecting the fine scale turbulence, the expansion of observational capabilities needed to describe the horizontal structure of these flows, etc. From a numerical modeling perspective, on the other hand, Saide *et al.* (2011) documented how the treatment of vertical and horizontal diffusion in the stable boundary layer of Santiago was of crucial importance in order to obtain better results in the numerical forecasting of PM concentrations. In-situ turbulence measurements like those documented here may help in validating and constraining the turbulence parameterizations used in numerical models. Considering the impact of this type of low-wind very stable boundary layers in the air quality problem of Santiago, addressing some of their theoretical, modeling and observational issues in this specific setting may constitute goals for further investigation.

ACKNOWLEDGMENTS

Personnel at the Dirección Meteorológica de Chile (DMC) is acknowledged for the installation and operation

of the 30-m meteorological mast. Mr. Raúl Inostroza from DMC is thanked for facilitating the access to the tower data. The comments and constructive suggestions of two anonymous reviewers are acknowledged.

DISCLAIMER

Reference to any companies or specific commercial products does not constitute endorsement.

REFERENCES

Arya, S.P. (1999). *Air pollution meteorology and dispersion*. Oxford University Press, 310 pp.

Barraza, F., Lambert, F., Jorquera, H., Villalobos, A.M. and Gallardo, L. (2017). Temporal evolution of main ambient $PM_{2.5}$ sources in Santiago, Chile, from 1998 to 2012. *Atmos. Chem. Phys.* 17: 10093–10107.

Barrett, B.S., Fitzmaurice, S.J. and Pritchard, S.R. (2012). Intraseasonal variability of surface ozone in Santiago, Chile: Modulation by phase of the Madden-Julian Oscillation (MJO). *Atmos. Environ.* 57: 55–62.

Corral, M. (2014). *Characterization of the thermal structure of the Santiago basin atmosphere and its relationship with air quality (in Spanish)*. M. Sc. thesis, Master Program in Meteorology and Climatology, University of Chile, 139 pp.

Escribano, J., Gallardo, L., Rondanelli, R. and Choi, Y.S. (2014). Satellite retrievals of aerosol optical depth over a subtropical urban area: The role of stratification and surface reflectance. *Aerosol Air Qual. Res*. 14: 596–607.

Garreaud, R. and Rutllant J. (2006). Meteorological factors of the air pollution in Santiago (in Spanish). In *Critical episodes of air pollution in Santiago*, Chapter 2, Morales, R. (Ed.). Editorial Universitaria, pp. 36–53.

Gramsch, E., Cereceda-Balic, F., Oyola, P. and von Baer, D. (2006). Examination of pollution trends in Santiago de Chile with cluster analysis of PM_{10} and ozone data. *Atmos. Environ.* 40: 5464–5475.

Gramsch, E., Cáceres, D., Oyola, P., Reyes, F., Vásquez, Y., Rubio, M.A. and Sánchez, G. (2014). Influence of surface and subsidence thermal inversion on $PM_{2.5}$ and black carbon concentration. *Atmos. Environ.* 98: 290–298.

Gramsch, E., Reyes, F., Vásquez, Y., Oyola, P. and Rubio, M.A. (2016). Prevalence of freshly generated particles during pollution episodes in Santiago de Chile. *Aerosol Air Qual. Res*. 16: 2172–2185.

Hogrefe, C., Hao W., Civerolo K., Ku, J.Y., Sistla, G., Gaza, R.S., Sedefian, L., Schere, K., Gilliland, A. and Mathur, R. (2007). Daily simulation of ozone and fine particulates over New York State: Findings and challenges. *J. Appl. Meteorol. Climatol.* 46: 961–979.

Jhun, I., Oyola, P., Moreno, F., Castillo, M.A. and Koutrakis, P. (2013). $PM_{2.5}$ mass and species trends in Santiago, Chile, 1998 to 2010: The impact of fuel-related interventions and fuel sales. *J. Air Waste Manage. Assoc.* 63: 161–169.

Jorquera, H. (2002). Air quality at Santiago, Chile: A box modeling approach - II. $PM_{2.5}$, coarse and PM_{10} particulate matter fractions. *Atmos. Environ*. 36: 331–344.

Jorquera, H. and Castro, J. (2010). Analysis of urban pollution episodes by inverse modeling. *Atmos. Environ*. 44: 42–54.

Kalnay, E., Kanamitsu, M., Kistler, R., Collins, W., Deaven, D., Gandin, L., Iredell, M., Saha, S., White, G., Woollen, J., Zhu, Y., Leetmaa, A., Reynolds, R., Chelliah, M., Ebisuzaki, W., Higgins, W., Janowiak, J., Mo, K.C., Ropelewski, C., Wang, J., Jenne, R. and Joseph, D. (1996). The NCEP/NCAR 40-year reanalysis project. *Bull. Am. Meteorol. Soc.* 77: 437–470.

Koutrakis, P., Sax, S.N., Sarnat, J.A., Coull, B., Demokritou, P., Oyola, P., Garcia, J. and Gramsch, E. (2005). Analysis of PM_{10}, $PM_{2.5}$, and $PM_{2.5\text{-}10}$ concentrations in Santiago, Chile, from 1989 to 2001. *J. Air Waste Manage. Assoc.* 55: 342–351.

Mahrt, L. (2007). Weak-wind mesoscale meandering in the nocturnal boundary layer. *Environ. Fluid Mech.* 7: 331–347.

Mahrt, L., Richardson, S., Seaman, N. and Stauffer, D. (2012). Turbulence in the nocturnal boundary layer with light and variable winds. *Q. J. R. Meteorol. Soc.* 138: 1430–1439.

Mahrt, L. (2014). Stably stratified atmospheric boundary layers. *Ann. Rev. Fluid Mech*. 46: 23–45.

Mullins, J. and Bharadwaj, P. (2015). Effects of short-term measures to curb air pollution: Evidence from Santiago, Chile. *Am. J. Agric. Econ.* 97: 1107–1134.

Muñoz, R.C. (2012). Relative roles of emissions and meteorology in the diurnal pattern of urban PM_{10}: Analysis of the daylight saving time effect. *J. Air Waste Manage. Assoc.* 62: 642–650.

Muñoz, R.C. and Undurraga, A. (2010). Daytime mixed layer over the Santiago Basin: Description of two years of observations with a lidar ceilometer. *J. Appl. Meteorol. Climatol.* 49: 1728–1741.

Muñoz, R.C. and Alcafuz, R. (2012). Variability of urban aerosols over Santiago, Chile: Comparison of surface PM_{10} concentrations and remote sensing with ceilometer and lidar. *Aerosol Air Qual. Res*. 12: 8–19.

Pérez, P. and Gramsch, E. (2016). Forecasting hourly $PM_{2.5}$ in Santiago de Chile with emphasis on night episodes. *Atmos. Environ.* 124: 22–27.

Ragsdale, K.M., Barrett, B.S. and Testino, A.P. (2013). Variability of particulate matter (PM_{10}) in Santiago, Chile by phase of the Madden-Julian Oscillation (MJO). *Atmos. Environ.* 81: 304–310.

Rasheed, A., Aneja, V.P., Aiyyer, A. and Rafique, U. (2015). Measurement and analysis of fine particulate matter ($PM_{2.5}$) in urban areas of Pakistan. *Aerosol Air Qual. Res*. 15: 426–439.

Reddy, P.J. and Pfister, G.G. (2016). Meteorological factors contributing to the interannual variability of midsummer surface ozone in Colorado, Utah, and other western US states. *J. Geophys. Res. Atmos.* 121: 2434–2456.

Rutllant, J. and Garreaud, R. (1995). Meteorological air pollution potential for Santiago, Chile: Towards an

objective episode forecasting. *Environ. Monit. Assess.* 34: 223–244.

Ryan, W.F., Piety C.A. and Luebehusen, E.D. (2000). Air quality forecasts in the mid-Atlantic region: Current practice and Benchmark skill. *Weather Forecasting* 15: 46-60.

Saide, P.E., Carmichael, G.R., Spak, S.N., Gallardo, L., Osses, A.E., Mena-Carrasco M.A. and Pagowski, M. (2011). Forecasting urban PM_{10} and $PM_{2.5}$ pollution episodes in very stable nocturnal conditions and complex terrain using WRF-Chem CO tracer model. *Atmos. Environ.* 45: 2769–2780.

Sax, S.N., Koutrakis, P., Ruiz-Rudolph, P.A., Cereceda-Balic, F., Gramsch, E. and Oyola, P. (2007). Trends in the elemental composition of fine particulate matter in Santiago, Chile, from 1998 to 2003. *J. Air Waste Manage. Assoc.* 57: 845–855.

Stull, R.B. (1988). *An introduction to boundary layer meteorology*. Kluwer Academic Publishers, 666 pp.

University of Santiago (2014). Update and systematization of the emissions inventory of air pollutants in the Metropolitan Region (in Spanish). Technical Report, 153 pp. http://www.sinia.cl/1292/articles-56914_Inf_Inventarios_FINAL.pdf.

Whiteman, C.D. (1990). Observations of thermally developed wind systems in mountainous terrain. In *Atmospheric processes over complex terrain*, Blumen, W. (Ed.), American Meteorological Society, 323 pp.

Wise, E.K. and Comrie, A.C. (2005). Meteorologically adjusted urban air quality trends in the Southwestern United States. *Atmos. Environ.* 39: 2969–2980.

Yegorova, E.A., Allen, D.J., Loughner, C.P., Pickering, K.E. and Dickerson, R.R. (2011). Characterization of an eastern US severe air pollution episode using WRF/Chem. *J. Geophys. Res. Atmos.* 116: D17306.

Yu, K.N., Cheung Y.P., Cheung T. and Henry, R.C. (2004). Identifying the impact of large urban airports on local air quality by nonparametric regression. *Atmos. Environ*. 38: 4501–4507.

Received for review, May 29, 2017
Revised, October 12, 2017
Accepted, October 19, 2017